

1 PROPERTIES OF CARBON NANOTUBES

There has been extensive research into the properties, synthesis and possible applications of carbon nanotubes (CNTs) since they came to prominence following the Iijima paper [1] of 1991.

1.1 THE STRUCTURE AND PROPERTIES OF THE CARBON NANOTUBE

Carbon nanotubes are composed of sp^2 covalently-bonded carbon in which graphene walls are rolled up cylindrically to form tubes. The ends can either be left open, which is an unstable configuration due to incomplete bonding, they can be bonded to a secondary surface, not necessarily of carbon, or they can be capped by a hemisphere of sp^2 carbon, with a fullerene-like structure [2]. In terms of electrical properties, single-walled CNTs can be either semiconducting or metallic and this depends upon the way in which they roll up, as illustrated in Fig. 1.1.

Multi-walled CNTs are non-semiconducting (i.e. semi-metallic like graphite) in nature. Their diameters range from 2 to 500 nm, and their lengths range from 50 nm to a few mm. Multi-walled CNTs contain several concentric, coaxial graphene cylinders with interlayer spacings of ~ 0.34 nm [3]. This is slightly larger than the single crystal graphite spacing which is 0.335 nm. Studies have recently shown that the intershell spacing can range from 0.34 to 0.39 nm, where the intershell spacing decreases with increasing CNT diameter with a pronounced effect in smaller diameter CNTs (such as those smaller than 15 nm) as a result of the high curvature in the graphene sheet [4,5]. As each cylinder has a different radius, it is impossible to line the carbon atoms up within the sheets as they do in crystalline graphite. Therefore, multi-walled CNTs tend to exhibit properties of turbostratic graphite in which the layers are uncorrelated. For instance, in highly crystallized multi-walled CNTs, it has been shown that if contacted externally, electric current is conducted through only the outermost shell [6].

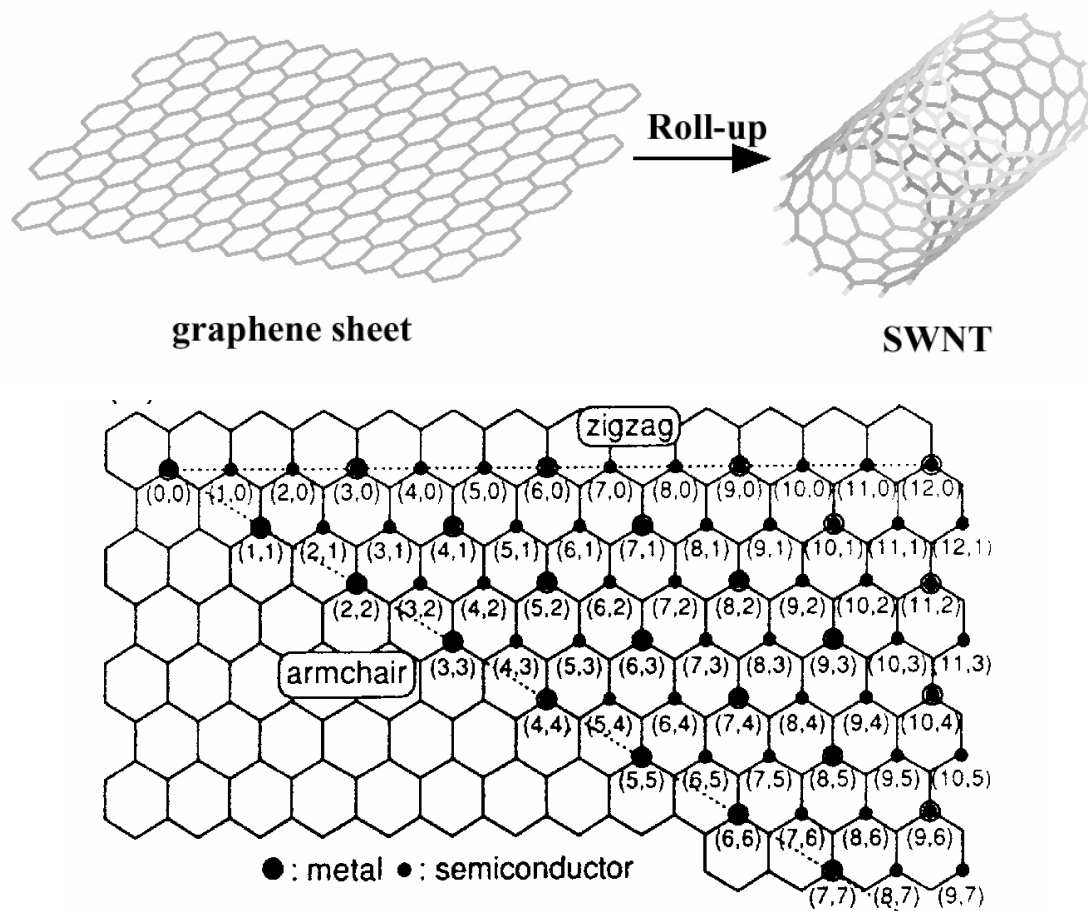


Figure 1.1: (top) A graphene sheet rolled up to obtain a single-walled CNT. (bottom) The map shows the different single-walled CNT configurations possible. Were the graphene sheet to roll up in such a way that the atom at (0,0) would also be the atom at (6,6), then the CNT would be metallic. Likewise, if the CNT wrapped up so that the atom at (0,0) was also the atom at (6,5), the CNT would be semi-conducting. The small circles denote semiconducting CNTs and the large circles denote non-semiconducting CNTs. Two thirds of CNTs are semi-conducting and one third metallic [7].

CNTs typically have a Young's Modulus ~ 10 times that of steel [8] and an electrical conductivity many times that of copper [9]. Some important properties of CNTs are listed in table 1.1.

Table 1.1: Properties of CNTs [12]

MECHANICAL PROPERTIES	
Young's modulus of multi-walled CNTs	~1-1.2 TPa
Young's modulus of single-walled CNT ropes	~1 TPa
Tensile strength of single-walled nanotube ropes	~60 GPa
THERMAL PROPERTIES AT ROOM TEMPERATURE	
Thermal conductivity of single-walled CNTs	1750-5800 WmK
Thermal conductivity of multi-walled CNTs	>3000 WmK
ELECTRICAL PROPERTIES	
Typical resistivity of single- and multi-walled CNTs	$10^{-6} \Omega\text{m}$
Typical maximum current density	$10^7\text{-}10^9 \text{ A cm}^2$
Quantized conductance, theoretical/measured	$(6.5 \text{ k}\Omega)^{-1}/(12.9 \text{ k}\Omega)^{-1}$
ELECTRONIC PROPERTIES	
Single-walled CNT band gap	
Whose n-m is divisible by 3	0 eV (metallic)
Whose n-m is non-divisible by 3	0.4-0.7 eV (semiconducting)
Multi-walled CNT band gap	~0 eV (non-semiconducting)

1.2 APPLICATIONS OF CARBON NANOTUBES

CNTs can be applied to many devices and technologies. Semiconducting single-walled CNTs have been investigated as transistors or logic elements [13-16]. The electronic properties of a single CNT in these devices varies greatly with adsorbed chemical species, which means they can be used as sensors [17, 18]. In highly crystallized CNTs, the coherent nature of electron transport can be used in spin-electronic devices [19]. They can also be used as electromechanical sensors as their electrical characteristics change upon structural mechanical deformation [20].

CNTs can be used as electrodes in electrochemical supercapacitors [21] because their structure leads to large surface areas with higher charge storage capabilities. The high electrical conductivity and the relative inertness of CNTs also make them potential candidates as electrodes for use in electrochemical reactions [22]. There has been

research into using CNTs to store hydrogen [23] though the amount stored is not as high as originally anticipated [24]. CNTs mechanically deflect upon electric stimulation which opens up the possibility of their application in cantilevers and actuators [21]. There has also been extensive work on their application in composites which utilize their physical strength and small size. Here single-walled CNTs are favoured as they are more flexible whilst still very strong [25].

In the near term, however, the CNT applications most likely to come to market first are their employment in various electron sources. There are three main types of electron emission: thermionic emission, field emission, or a mixture of the two. The next section will focus on the various applications of electron sources, which type of emission they use and their relative merits together with an in depth look at field emission.

1.3 ELECTRON EMISSION APPLICATIONS

Electron sources are employed in a wide range of technologies which include displays [26], telecommunication devices [27], electron-beam imaging equipment [28] and microwave amplifiers [29]. The most widely employed electron source is still the thermionic cathode used in television cathode-ray tubes and high-power microwave amplifiers, though its popularity is on the decline with the advent of flat-panel displays. Thermionic emission occurs when a charged metal or a charged metal oxide surface is heated. The thermal vibrational energy gained by the electrons overcomes the electrostatic forces holding them to the surface. The electrons are released into vacuum from the surface and the resultant beam is controlled by a sequence of fields. The temperature of operation is typically 2000 K: an undesirable requirement as this results in an inefficient consumption of power. Though you can get thin CRTs at present, the vacuum tube required is typically quite large, which has also contributed to its decline in popularity. Demand has pushed the requirements of the electron source to smaller and smaller scales to increase efficiency and to open up opportunities for alternative electron source applications. As well as flat-panel displays, new applications include parallel electron-beam microscopy and

nanolithography, compact microwave amplifiers and portable X-ray tubes. These applications have motivated worldwide research into alternative smaller, more efficient electron source technologies.

Field emission, also known as Fowler-Nordheim tunnelling, is a form of quantum mechanical tunnelling in which electrons pass through a barrier in the presence of a high electric field (as shown in figure 1.3). Field emission offers a route to smaller, more efficient electron source technologies. The phenomenon is highly dependent on both the properties of the material and the shape of the cathode; high aspect ratios produce higher field emission currents.

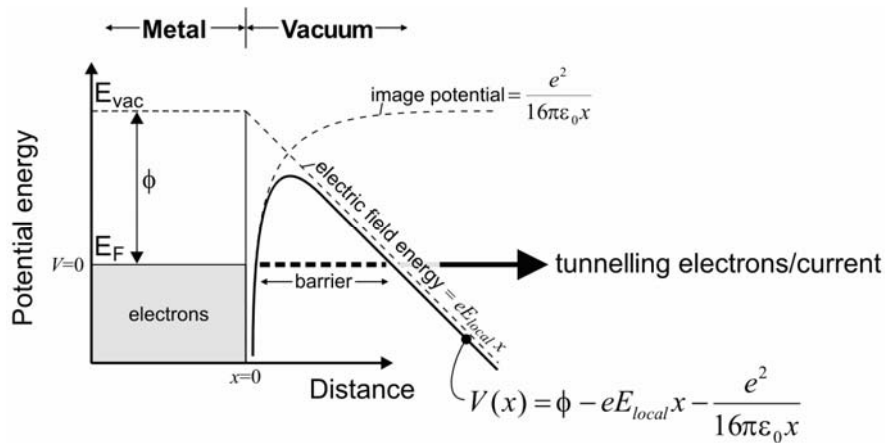


Figure 1.3: A diagram representing the band structure showing the tunnelling of free electrons at the Fermi level (for a metal-like material) through an electric field-narrowed potential barrier [30].

In contrast to the commonly used thermionic emission based on a hot filament, field emission occurs at or close to room temperature from an unheated ‘cold’ cathode under the influence of an electric field. Consequently, field emitters are more power-efficient than the heated thermionic emitter. Also, field emission sources offer several attractive characteristics such as instantaneous response to field variation, resistance to temperature fluctuation and radiation, a high degree of coherence in electron optics, a good on/off ratio, ballistic transport and a nonlinear current-voltage relationship in which a small change in voltage results in a large change in emission current.

However, to extract a current significant enough to be used for the aforementioned applications, field emission requires a very large local field of a few V/nm. A typical method employed to attain this high field is to use a very sharp needle, such as tungsten, with the apex chemically etched to a few hundred nanometres. Even so, with this geometry, a few thousand volts still needs to be applied macroscopically in order to draw a useable current (eg. the extraction voltage of a field emission electron microscope is 1-5 kV). Field emission will be discussed in greater detail later in this section.

1.3.1 MOTIVATION FOR CARBON NANOTUBE EMITTERS

Much research has been focused on the application of CNTs to field emission sources because they have several advantages over other field-emitting materials.

Firstly, when compared with other commonly used emitters such as tungsten, the CNT's covalent bonds are much stronger than tungsten's metallic bonds. As a result, the activation energy for surface migration and diffusion of the emitter atoms is much larger than for a tungsten electron source, making it much more unlikely. Therefore, the tip can withstand the extremely strong fields (several V/nm) needed for field emission. Related to this point, nanotubes can be very stable emitters, even at high temperatures. Purcell et al [31] demonstrated that a multi-walled carbon nanotube emitter could be heated by its field-emitted current up to 2000K and remain stable. They claimed that this was the first reported observation of field emission induced stable heating. This characteristic is distinctly different from metal emitters. In metals, the resistance, R , increases with temperature, which means that more heat, Q , is produced as higher currents, I , are drawn ($Q = I^2R$). The combination of high temperature and electric field causes the well known mechanism of field-sharpening of tips by surface diffusion, which in turn increases the local field, current and temperature. This positive feedback mechanism causes an unstable thermal runaway which inevitably leads to emitter destruction for metal-based emitters. In contrast, the resistance of a nanotube decreases with temperature which limits I^2R heat generation. Consequently, its temperature varies sub-linearly with current.

Secondly, when compared with other film field emitters such as diamond or amorphous carbon structures, CNTs have a high aspect ratio, a small radius of curvature of the cap and good conductance [32]. Utsumi [33] evaluated commonly used field emission tip shapes as shown in Figure 1.3.1, and concluded that the best field emission tip should be whisker-like, followed by the sharpened pyramid, hemispheroidal, and pyramidal shapes. Indeed, nanotubes are whisker-like. It has been reported that even curly ‘spaghetti-like’ nanotubes stand up vertically like whiskers during emission under the application of an electric field [34].

Thirdly, because of the CNT’s extremely large Young’s modulus and maximal tensile strength, they are able to withstand the high fields around them and current densities coming from within.

Fourthly, the graphene walls in them are parallel to the filament axis resulting in the nanotubes (whether metallic single-walled or multi-walled) exhibiting high electrical conductivity at room temperature.

Finally, carbon has one of the lowest sputter coefficients [35], which is an advantage as an electron source is usually bombarded by positive ions.

Classification and ranking of tip-shapes for field enhancement [39]:

- (a) rounded whisker
- (b) sharpened pyramid
- (c) hemi-spheroidal
- (d) pyramidal

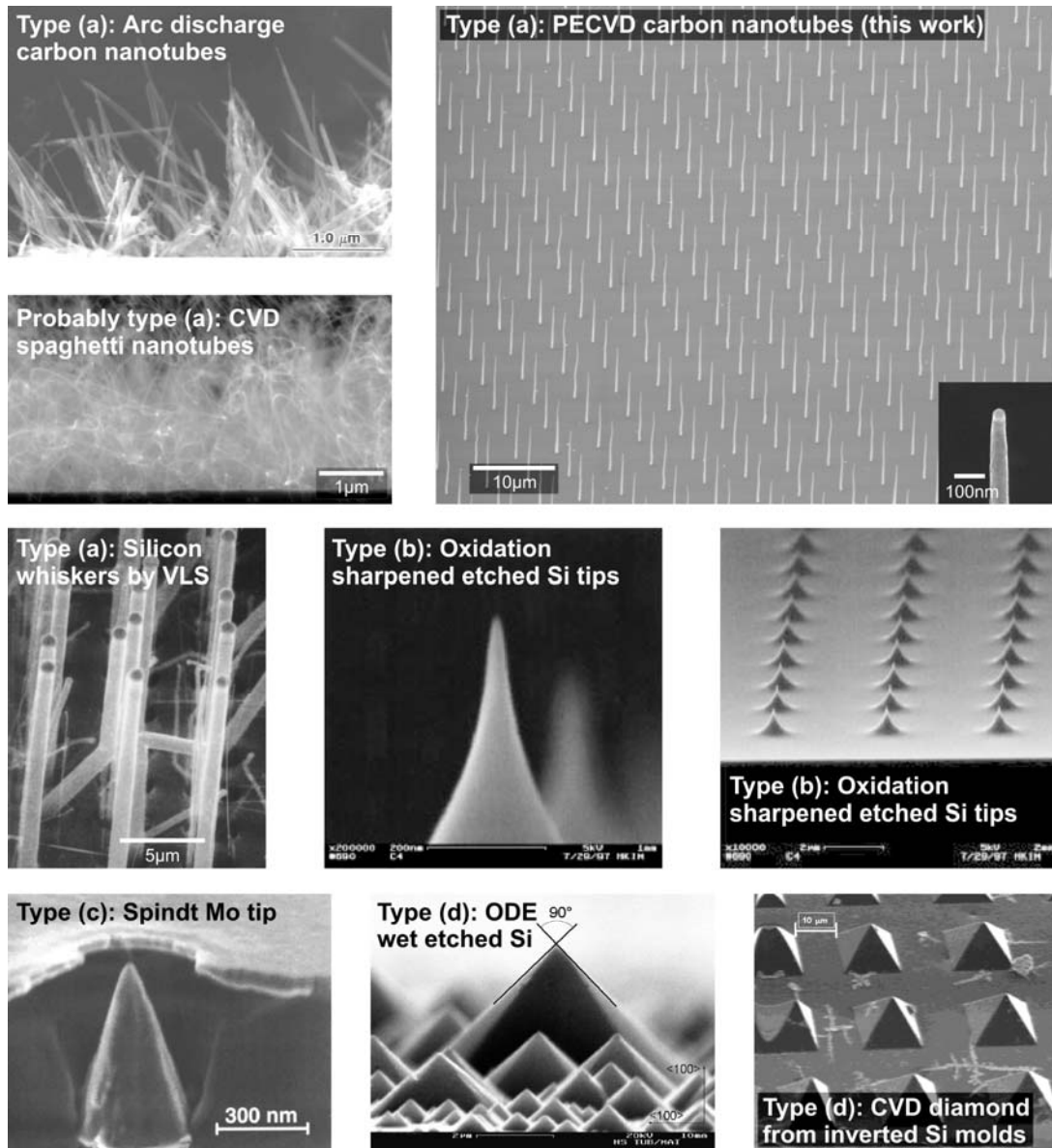
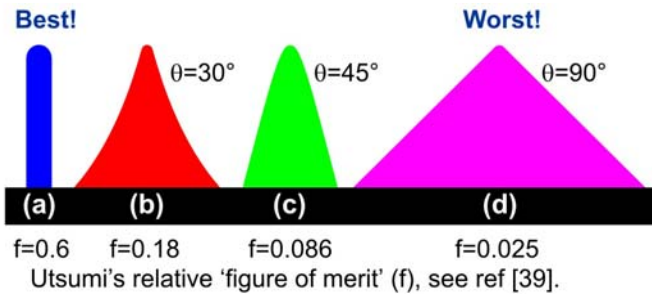


Figure 1.3.1: Classification and ranking of tip-shapes proposed by Utsumi[33]. From best to worst - (a) rounded whisker which is ideal, (b) sharpened pyramid, (c) hemi-spheroidal, and (d) pyramidal [35].

1.3.2 CARBON NANOTUBE FIELD EMISSION APPLICATIONS



Figure 1.3.2: Applications, such as lamps, X-ray source and field emission displays, using carbon nanotubes (CNT) as the field emission electron source [36].

Research groups have recently been focusing on the controlled production of micro-field emission sources based on carbon nanotubes. Such electron sources could be used in microguns for electron microscopy and parallel electron beam lithography, but are also equally applicable to ‘macroscopic’ applications such as field emission displays, microwave amplifiers and X-ray sources. Examples of these are shown in figure 1.3.2. This thesis focuses on their use as sources in electron microscopy, but other applications will be outlined first.

1.3.2.1 FIELD EMISSION DISPLAYS

The application area of CNT electron sources with the largest potential market is the flat-panel field-emission display [37, 38], which provides a high-brightness display for both consumer and professional applications. Figure 1.3.2.1 shows the functions of the simplest form of a display pixel. Nanotubes are patterned on a matrix of electrodes in a vacuum housing. The counter electrode is a glass plate coated with a conducting but transparent layer and a phosphor layer. A voltage difference of a few kilovolts between the nanotube cathode and the glass plate results in field emission and the generation of light through excitation of the cathodoluminescent phosphor. An image can be obtained by addressing selectively the different positions of the matrix, which can either be monochrome or in colour if each pixel is divided in red, blue and green sub-pixels.

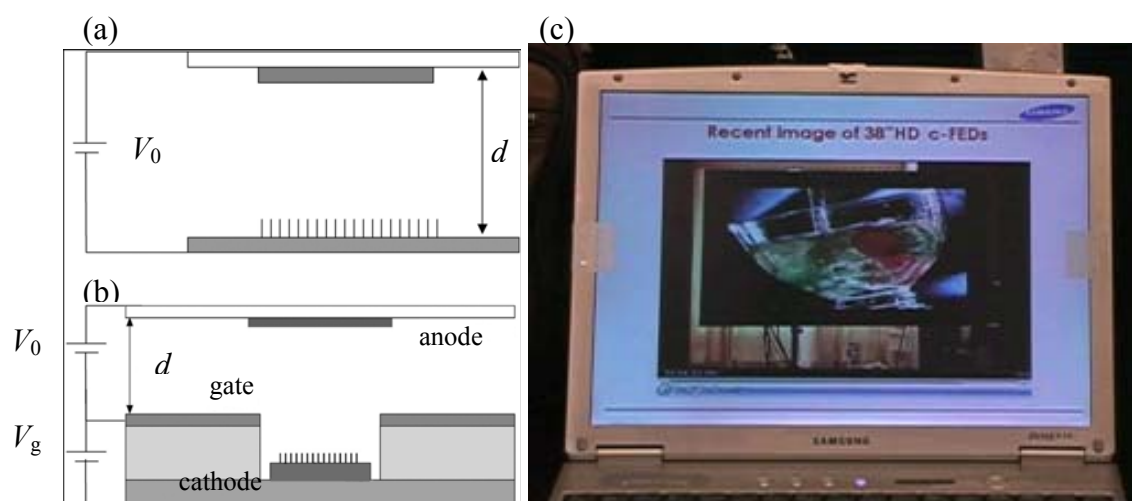


Figure 1.3.2.1: Schematic of the working principle of a field-emission display pixel: (a) diode structure; (b) triode structure with ballast resistor in series with the emitters; (c) image of a prototype of a CNT field-emission display [39] with a gate structure, an active area of 38" in diagonal, full colour and 100 Hz.

Problems include the large voltage difference required between the cathode and the anode to operate the display, which is needed both for extracting electrons and to maximize efficiency in the phosphor. Also, it is probable that each pixel requires a different gate voltage and so every pixel must be current regulated individually to

obtain stable emission. CNTs incorporated directly onto the electrodes are likely to degrade. CNTs would need lifetimes of several years on the electrode for the display to be viable.

1.3.2.2 CARBON NANOTUBES APPLIED TO GATED CATHODES FOR PARALLEL ELECTRON BEAM LITHOGRAPHY

If the same principle used in field emission displays is applied to electron beam lithography, but with only one CNT as an electron source, then an array of parallel gates could be used to speed up parallel-write electron beam lithography. With several electron beams acting in parallel, this would vastly decrease the time it takes to write electron beam patterns onto silicon chips with lithography. It would also enable an increase in resolution because CNTs tend to be smaller than typical electron sources used for lithography. Figure 1.3.2.2 shows what a typical array of electron sources might look like.

Carbon nanotubes are an ideal electron source for such a novel parallel e-beam lithography system, but currently, more work is still needed to increase the yield of functioning cathodes.

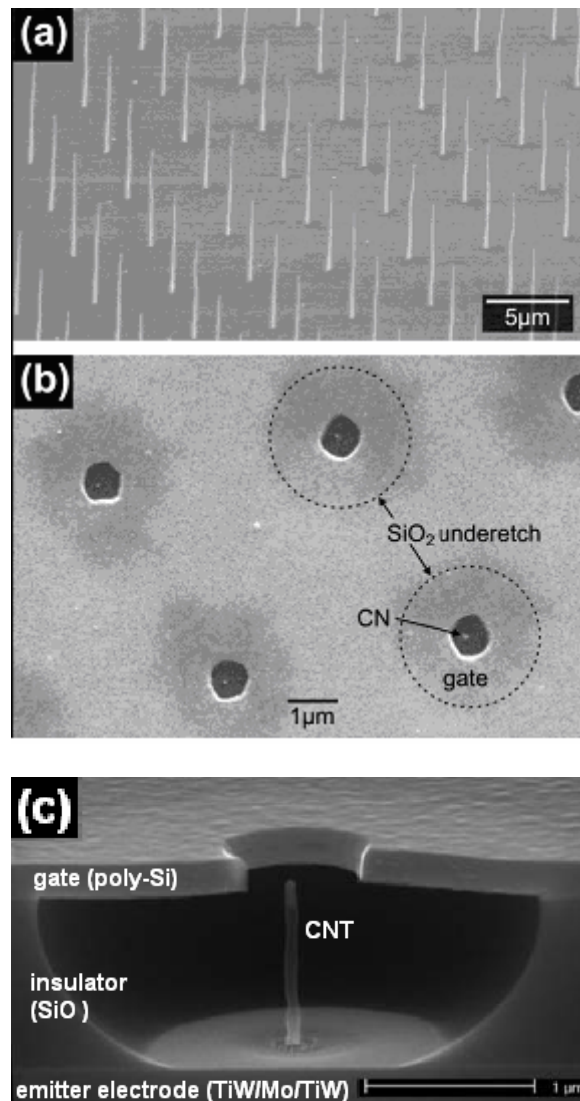


Figure 1.3.2.2: (a) An array of carbon nanotubes, with a 5 μm pitch. (b) Top view of the integrated gate carbon nanotube cathode. The pitch of the gate apertures is 5 μm . The nanotube appears as a bright dot in each gate aperture. (c) Cross section SEM view of the integrated gate carbon nanotube cathode, showing the gate electrode, insulator, emitter electrode, and vertically standing nanotube [40].

1.3.2.3 CARBON NANOTUBES AS COLD MICROWAVE AMPLIFIERS

Current microwave amplifiers use electron sources that operate thermionically and use a lot of power. An alternative method for microwave amplification reported recently [41] incorporates a microwave diode that instead uses a cold-cathode electron

source consisting of a CNT array which operates at high frequency and at high current densities. As field emission sources are smaller and weigh less, the reduction in power and mass would make satellite transponders much cheaper.

1.3.2.4 OTHER FIELD EMISSION APPLICATIONS

Field emission from CNTs has been employed in X-ray sources [42], where a film of CNTs is used as the cathode. They have also been employed in field emission lamps [38], where CNTs are again used as a cathode. They can also be used as an emitting CNT in an electrically driven mechanical resonator [31], and high precision thrusters for space telescopes [43].

1.4 ELECTRON GUN SOURCES

Electron microscopy demands a bright, stable, low-noise electron source with a low kinetic energy spread in order to maximise spatial resolution and contrast. Recent research, detailed later in this section, has investigated whether the carbon nanotube can act as an improved electron source for this application and how it compares to the best electron sources available today.

1.4.1 CURRENT MICROSCOPY ELECTRON SOURCE TECHNOLOGY

An electron gun is the source of electrons in the electron microscope. Figure 1.4.1 shows a typical microscope with the source denoted. The beam is focused by a system of lenses and then rastered across a sample by a quadrupole. Either secondary electrons are detected above the sample as in a scanning electron microscope (SEM) or transmitted electrons are detected on the other side of the sample as in a transmission electron microscope (TEM). The quality of all these components

ultimately determines the quality of the image obtained from an electron microscope, and manufacturers are continually addressing these factors to improve resolution.

The quality of the electron source itself is a contributing factor. The source's various attributes combined determine the resolution a microscope can attain. These are: the stability of the electron beam, the kinetic energy spread of electrons within the beam, the virtual source size (which is related to the area on the tip that the electron are emitted from), and the reduced brightness which determines how much current can be extracted for a given voltage. These will be discussed in greater detail later in the chapter.

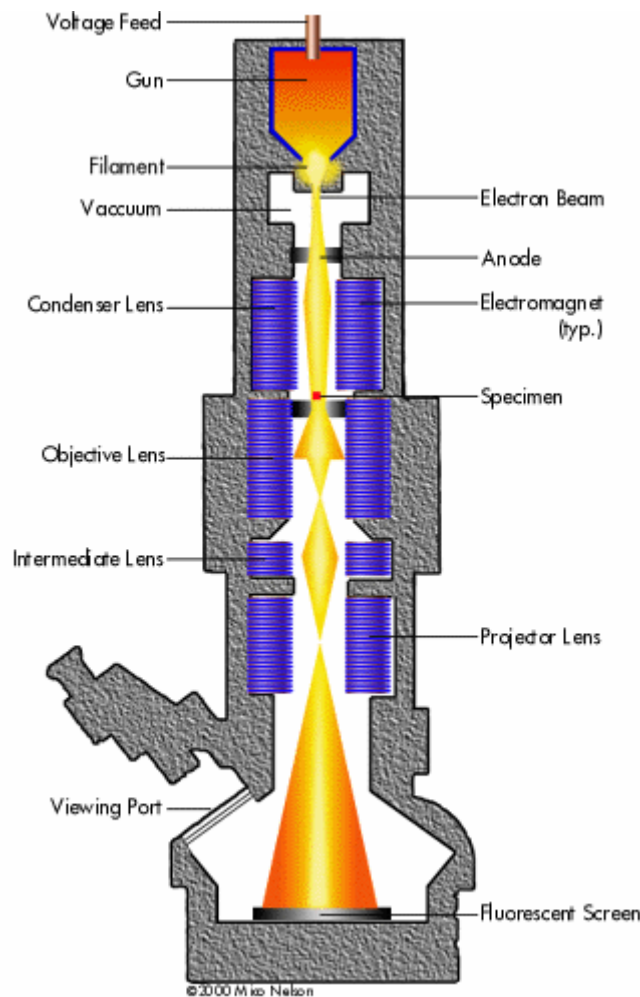


Figure 1.4.1: Schematic cross-section of a typical electron microscope. The electron source is inserted into the area marked 'gun,' a voltage or power source applied and an electron beam extracted by the anode.

Different electron sources can be used to maximise one or two of these attributes, sacrificing the others when targeted towards a particular application. These properties are material-dependent and the various electron sources currently available on the market are discussed below [44, 45].

1.4.1.1 LANTHANUM HEXABORIDE EMITTERS

LaB₆ emitters were the first to be commonly used in electron microscopy. LaB₆ emitters are cut from a larger single crystal. They have a long lifetime (~2000 hours), are very stable, bright and have a low workfunction of 2.4 eV. They operate thermionically, in the same way that tungsten does and can be tailored to certain applications during the fabrication process. They are typically used as electron sources for e-beam lithography.

Fabrication commonly involves zone-refining followed by fine-cutting the crystal into a piece of the desired size. This is then attached to a tip by either braising or by being ‘squeezed’ between two supporting prongs as shown in figure 1.4.1.1. The angle subtended at the apex of the tip, the cone angle, is formed by grinding. For applications such as TEM where a high-resolution beam is required, the cone angle is ground to 60° (hence quite steeply inclined to the axis) leaving a very small area on top of the tip from which electrons can be emitted. However, for applications such as E-beam lithography, a very stable source is required; hence quite a flat cone angle of 90° is used, which results in a large area on the top of the tip from which electrons emit. Obviously, this compromises resolution.



Figure 1.4.1.1: A typical LaB₆ electron source. The LaB₆ is the purple crystal in the centre and is supported under compression with graphite.

LaB₆ emitters, however, are becoming less popular. They commonly have a large energy spread of 1 eV and are not very bright (10^7 A/cm²SR). Customers purchasing electron microscopes often opt for tungsten thermionic emitters even though they have much shorter lifetimes.

1.4.1.2 THE TUNGSTEN THERMIONIC EMITTER

Tungsten thermionic emitters in essence have virtually the same properties as LaB₆. However, tungsten emitters only last for ~100 hours, whereas LaB₆ emitters can last for months. They also have a large source size ($>10^4$ atoms) due to their shape, and are even less bright than LaB₆ emitters (10^6 A/cm²SR).

However, they are favoured because of their simplicity of manufacture. The emitter consists of a wire filament bent into the shape of a hairpin which is attached to a thicker metal support (see figure 1.4.1.2). The filament operates at ~2700 K by resistive heating. The tungsten cathodes are widely used because they are both reliable and inexpensive. Lateral resolution is limited because the tungsten cathode current densities are only about 1.75 A/cm².

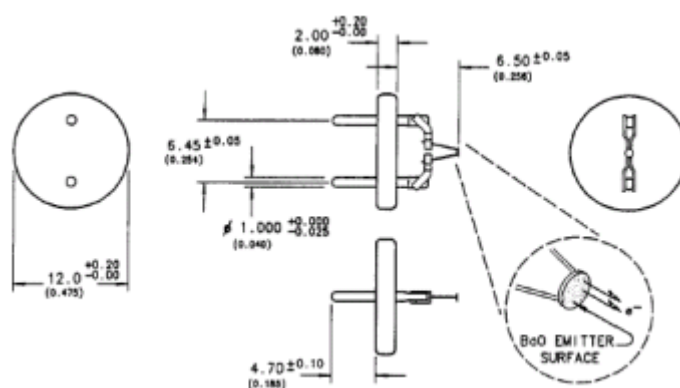


Figure 1.4.1.2: A schematic diagram of a typical tungsten hairpin thermionic emitter (courtesy of Barry Scientific Inc, Fiskdale, MA, USA). The hairpin is quite large, which results in electron emission coming from a very large area. Consequently, the resultant current is relatively weak.

The fabrication of a LaB₆ emitter is more convoluted, so this will increase the price. The other advantage of the tungsten emitter over the LaB₆ emitter is that the latter can often fall off as it is only held by pressure.

1.4.1.3 THE SCHOTTKY EMITTER

The Schottky emitter is made out of single crystal tungsten and is coated with a thin layer of zirconium oxide. Zirconium oxide is added to the tungsten tip to reduce the workfunction. A low workfunction is desirable, as this will result in a low kinetic energy spread at high temperatures. It is designed to operate within definite temperature boundaries over time. The range is typically 1750-1800 K. The source size is typically 15 nm, the energy spread low ~ 0.3 eV. It is brighter than both thermionic emitters with a typical brightness of 5×10^8 A/cm²SR and has a stability of less than 1%. They also last a very long time (1-2 years is typical). Interestingly, Schottky emitters increase in noise with time (the timeframe being over the period of a year). The mechanics of this are not yet clearly understood.

A single crystal tungsten wire, typically of 100 μ m diameter and 5 mm long is spot-welded to a tungsten crosswire of similar dimensions which in turn is attached to two thick covar (a metal alloy) prongs, as shown in the schematic in figure 1.4.1.3.1. It is vitally important in this process that all parts of the electron column, especially the electron source are aligned along a single beam-axis. Consequently, many checking steps are carried out during the fabrication process. Tips that are not aligned to within 2 μ m of the vertex of the crosswire are discarded.

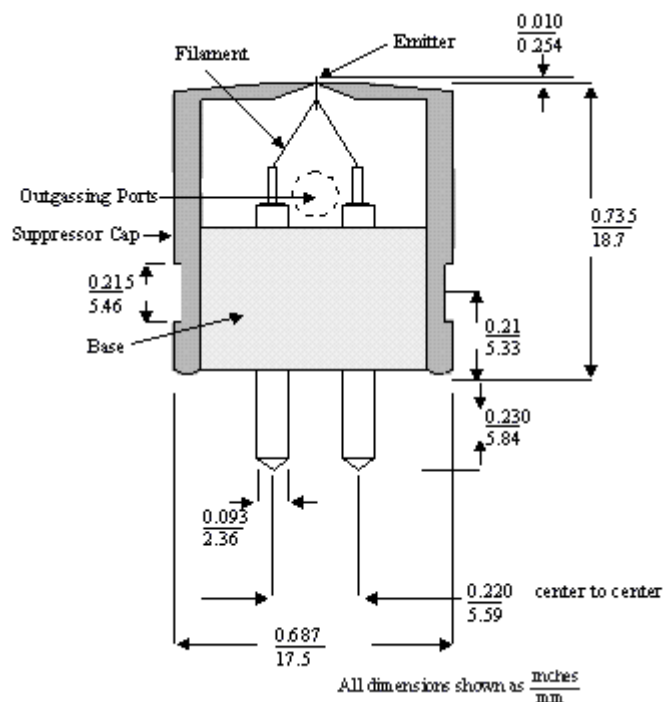


Figure 1.4.1.3.1: Schematic of a tip made at FEI in Oregon. The ceramic base holds two metal prongs, with a crosswire connecting the two. At the vertex of the crosswire, the tip is attached. This should be attached with the whole shaft of the tip centrally located on-axis so it can be aligned with the rest of the column. The suppressor (in dark grey) is also shown on this diagram. It is fixed to the ceramic base by grub screws under compression.

To obtain a sharp tip, the tip is inverted and etched in NaOH solution. There are various factors that can affect the repeatability of this process, so it is important to minimise the effect of these factors. For instance, the temperature of the solution must remain constant. Therefore, the etchant is placed in a bath which can control the temperature to the nearest °C. Air and solution currents can also affect the etching as can the depth to which the wire is held below the meniscus of the solution and the etchant concentration. There are also two etching stages to maximise repeatability. Tips produced at FEI typically measure 150 nm across with a constantly maintained cone angle. Once etching is complete, the remnants of sodium hydroxide are removed by dipping in alcohols and boiling water. This step must be highly repeatable, so great care is taken to ensure that all experimental parameters are kept constant. The tip is then mounted in a gun module.

The next step involves the addition of zirconium to the tip. This is done by daubing on zirconium hydride. The zirconium hydride is ground into a fine powder, and water added to form a slurry so it is spreadable in the schematic in figure 1.4.1.3.2.

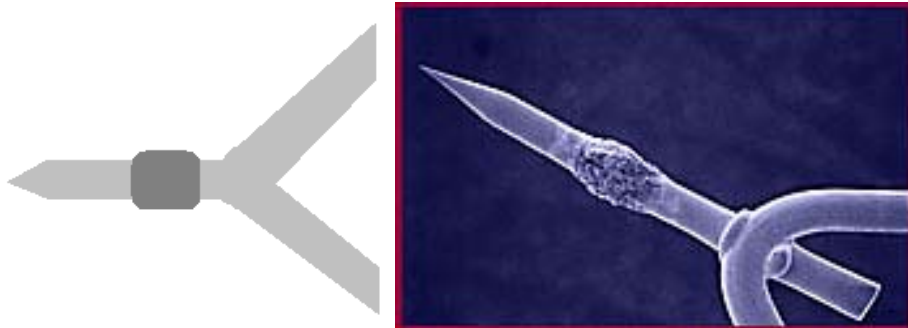


Figure 1.4.1.3.2: *Left*, a zirconium hydride blob daubed onto a tungsten wire. The amount deposited must be large enough to give the emitter a lifetime of over a year, but small enough so that the supply to the tip is controlled. *Right*, an electron microscope image of a typical tip.

The tip is then transferred to a chamber where approximately 40 tips are heated to 1800 K simultaneously under vacuum whilst suspended upside down (as electron sources commonly are in electron columns). Under heating, the hydrogen is liberated and oxygen is added to form ZrO. This diffuses through surface tension to the end of the tip where a thin layer of ZrO forms. This gives the ZrO Schottky emitter. Zirconium evaporates in the vacuum. However, this is always replaced as the zirconium acts as a reservoir. So, there is a constant movement under surface tension of zirconium moving down the tip. Hence the tip has stable characteristics over a very long time.

1.4.1.4 COLD FIELD EMITTERS

The main benefits of cold field emitters are a small virtual source size (typically of 3 nm in tungsten), a low energy spread of 0.2-0.3 eV, high brightness 10^9 A/cm²SR and a lifetime of over a year. These field emitters are commonly used in high resolution electron microscopes as they are bright and the kinetic energy spread is low. Tungsten is the most commonly used cold field emitter, but its major disadvantage is its poor

stability, which has been said to be as much as 6%. That said, there is confusion over what “stability” means. This will be discussed in further detail in chapter four. The reason for poor stability is the metallic nature of the bonding in tungsten. Metallic bonds are not as strong as ionic or covalent bonds. Upon application of a high electric field, atoms on the tungsten tip can move around the tip, thus changing the shape of the tip which results in alteration of the field which in turn leads to current oscillation.

The tungsten tips are fabricated using the same method as in Schottky emitters, though etch conditions will be changed to obtain tips that are 40 nm in radius. It is desirable to find a field emitter that is more stable over long periods.

1.4.2 TIP CHARACTERISATION

All tips sold by the electron beam industry are characterised prior to delivery. Tips are mounted in a suppressor and extractor setup, and then fitted into a gun module for testing (complete with Faraday cup). All the important properties of the emitter are determined and included on a datasheet for each tip. The properties of all the tips discussed are summarized in a table 1.4.2.

Table 1.4.2: A summary of the various types of electron source. The cold field emitter refers to tungsten and the tungsten emitter values refer to its thermionic properties [44,45].

	Schottky	Cold Field	LaB ₆	Tungsten
Source size (nm)	15	3	10 ⁴	> 10 ⁴
Energy spread (eV)	0.3-1.0	0.2-0.3	1.0	1.0
Brightness (A/cm ² SR)	5 × 10 ⁸	10 ⁹	10 ⁷	10 ⁶
Short-term stability %	< 1	4-6	< 1	< 1
Service life	> 1 year	> 1 year	2000 hours	100 hours
Workfunction (eV)	~2.3	~4.5 eV	~2.5 eV	4.5 eV

Characterisation takes about 10 minutes per tip, so to increase efficiency 10 are done in one cycle which is one of the benefits of scaling a process up to factory production. As an indication of the numbers involved, FEI Company typically manufacture 100 Schottky emitters a week with approximately 70 % considered fit for sale.

1.4.3 TIP ALIGNMENT

It is important to have alignment of the tip, as any error in the beam alignment will be magnified through all the various lens corrections down the column. This is a major cause of astigmatism. Alignment is checked using a simple microscope with a large screen projection. The axis alignment is tested first. The tip, commonly sitting on a crosswire attached to prongs through a ceramic (see figure 1.4.1.2), is placed in a simple stand horizontally and rotated through 360°. The extremities of deviation are noted and if the range of the deviation is greater than 2 μm , the tip is discarded.

The tip is exposed to high temperatures and current throughout the tip's life, which for the case of the Schottky emitters, can be years. As a consequence, the shape and structure of the tip is likely to change over this time and it is desirable to know the extent of such changes. Therefore, many measurements of the tip's dimensions are made using this simple microscope setup (as it can measure to the nearest 10,000th of an inch) to see the change after the tip has been used for some time.

1.4.4 ALIGNMENT IN THE COLUMN

The whole electron column is specifically designed so that everything slots into place. The column is designed so that there is a manoeuvrability of about 5 μm to ensure that lenses, electron sources and differential pumps are aligned so that the electron beam can travel through to the sample without deflection. Differential pumps consist of a small hole or tube whose dimensions are determined by a set of equations that determine flow rates between chambers at different pressures. For instance, the electron source itself is commonly at 10^{-9} mBar, the electron column at 10^{-7} mBar, and

the sample chamber 10^{-6} mBar. It typically takes 3-5 days to construct a completely new column and make it fully operational.

1.5 FIELD EMISSION PROPERTIES OF CARBON NANOTUBES

It is straightforward to see how CNTs are good candidates for standard field emission applications used in displays, but it is important to understand in more detail why carbon nanotubes are desirable for high-quality field emission sources. Only recently has detailed research into field emission from nanotubes been carried out. Amongst the first to look into nanotube field emission properties was Martijn Fransen whose thesis [46] included detailed investigations and comparisons of the materials used for field emission in electron guns currently available. In the final chapter, he found a source that was as bright as the ZrO Schottky emitter (which is considered to be the brightest electron gun material available at the moment), yet a more stable source with a significantly lower kinetic energy spread than the W emitter, currently used to obtain higher resolutions.

Further and much more detailed investigations were carried out by de Jonge et al [47]. As well as determining the typical characteristics of field emitters such as brightness, kinetic energy spread etc, it was also important to conclusively determine whether the emission was coming from the nanotube itself. This section will outline Fowler-Nordheim theory and will detail the various properties of electron beams which are used to determine the feasibility of electron sources and discuss whether the CNT is a viable alternative source.

1.5.1 FOWLER-NORDHEIM THEORY

Field emission is the quantum-mechanical tunnelling of electrons from a surface into vacuum in response to a very high electric field. In a material, electrons at the Fermi level must overcome the potential barrier imposed by the workfunction, ϕ , before they can escape into vacuum. In the presence of an external electric field, the external

potential barrier $V(x)$ is modified as shown in Figure 1.3. For typical metals ($\phi \sim 4.5$ eV), field emission occurs when the barrier width is reduced to a few nanometres under an applied electric field, E_{local} , of a few V/nm. Due to the quantum-mechanical uncertainty in the electron position, electrons are able to tunnel across this narrow barrier. As the field increases, the barrier width decreases resulting in more electrons tunnelling across the barrier. Typically, detectable tunnelling current occurs where $E_{local} > 3$ V/nm.

For any material, the tunnelling current density is given by integrating the product of the electron transmission probability through the barrier, $T(E)$, and the incident supply of electrons, $N(E)$, over the range of potential energies. Physically, $T(E)$ depends on the barrier width, which in turn depends on the field applied and the work function of the material. $N(E)$ depends on the band structure of the material and the distribution of electrons at a particular temperature. By assuming a metallic free-electron band structure at 0 K, the variation of current with field from a field emitter is dictated by the Fowler-Nordheim (FN) theory of field emission [48], where the current density J can be expressed as:

$$J = c_1 \frac{F^2}{b_1^2 \phi} \exp\left\{a_2 c_2 c_3 \frac{1}{\sqrt{\phi}}\right\} \exp\left\{-a_1 c_2 \frac{\phi^{3/2}}{F}\right\} \quad \text{Eq. 1.5.1.1}$$

with workfunction ϕ and electric field F . The constants were determined elsewhere [49] and defined as

$$a_1 = 0.958$$

$$a_2 = 1.05$$

$$b_1 = 1.05$$

$$c_1 = e^3/8\pi h$$

$$c_2 = 8\pi\sqrt{(2m)/3}he$$

$$c_3 = e^3/4\pi\epsilon_0$$

with the electron charge e , Planck's constant h , electron mass m and the permittivity of free space ϵ_0 taking their usual values. The local field at the apex of a sharp,

electrically conducting tip equals the product of the extraction voltage U and the field enhancement factor β :

$$F = \beta U \quad \text{Eq. 1.5.1.2}$$

The value of β can be computed numerically if the geometry of the emitter [48] is known.

A graph of $\log I/U^2$ versus $1/U$, the FN plot, is therefore a linear curve. This was found to be the case when field-emission measurements were taken of nanotubes attached to tips. De Jonge et al. repeated the measurements for eight tips, (the first of which is shown in Figure 1.5.1). TEM images of the nanotubes had found that most CNTs had a few walls and a radius of between 1 and 3 nm, which was consistent with the values that they obtained from the FN plots.

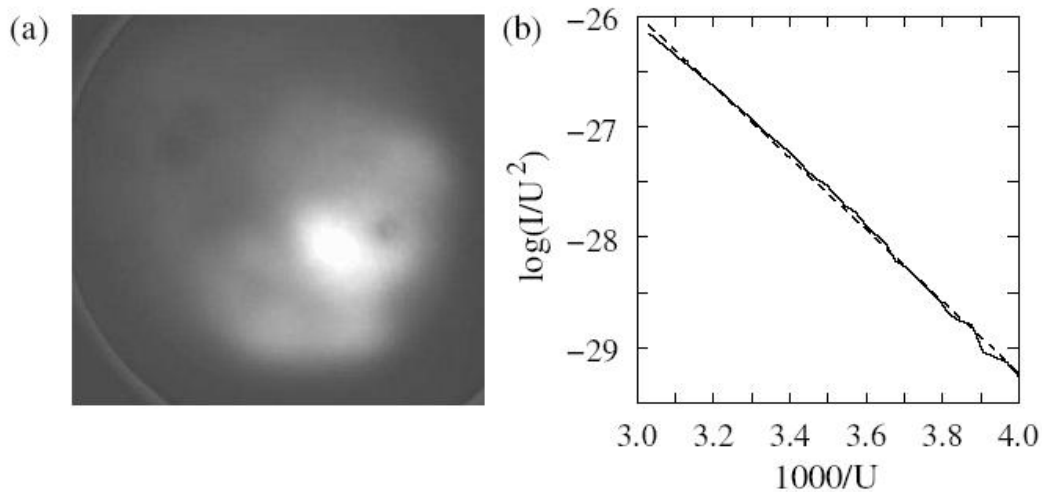


Figure 1.5.1: Emission measurements of a typical CNT electron source for $T = 800$ K in a vacuum of 3×10^{-10} mBar. (a) Field emission pattern recorded with a micro channel plate and a phosphor screen. (b) FN plot and a linear fit with a slope of -3244 (dashed). Figure courtesy of de Jonge.

1.5.2 MEASUREMENT OF THE ENERGY SPECTRUM

The current density function $J(E)$ as a function of the energy E is given by:

$$J(E) \propto \frac{\exp\left(\frac{E}{d}\right)}{1 + \exp\left(\frac{E}{k_b T}\right)} \quad \text{Eq. 1.5.2.1}$$

where k_b is the Boltzmann constant, T is the temperature and d , the tunnelling parameter, given by:

$$d = \frac{c_4 F}{b_1 \sqrt{\phi}} \quad \text{Eq. 1.5.2.1}$$

where the constants are:

$$c_4 = eh/4\pi\sqrt{2m}$$

$$k_b = 1.3806 \times 10^{-23} \text{ J/K}$$

The energy spread, ΔE , of the emitted electron beam is usually expressed by the full width half maximum of the energy spectrum. The width of the low-energy side of the energy spectrum is determined by the tunnelling parameter, d , whilst T sets the width of the high-energy side.

To measure the kinetic energy spread of the electrons emitted, the use of a retarder is required. To achieve a high resolution to take these measurements, a system of plates and lenses is required (see figure 1.5.2.1).

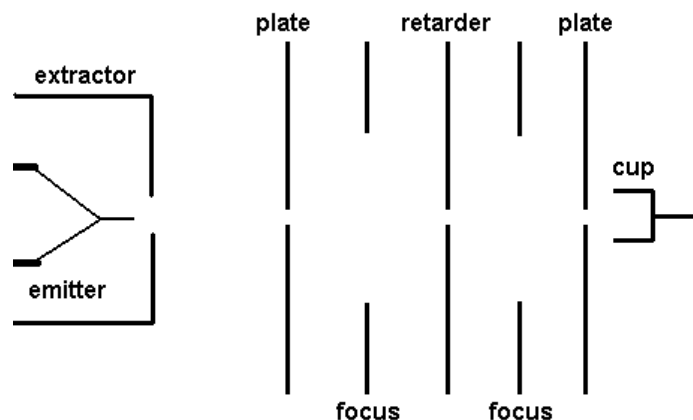


Figure 1.5.2.1: A schematic of the energy spread measurement setup courtesy of FEI Company. Electrons emitted due to the extractor move towards the plate which is at the same potential as the extractor (in order not to alter the path of the electrons since electrons moving with different energies will be moved by different amounts). The focus lenses are typically 0.95-0.97 the potential of the tip and this depends on the design. The retardation voltage varies either side of the set high voltage by a ramping voltage to cover the energy spectrum. Once the electrons get through the hole, and if the ramp and retarder voltages are nearly equal, then the focus lens on the other side will reaccelerate the electrons to get through to the cup.

Effectively, the number of electrons that get through is counted. This will obviously be very low for high retardation potentials, and very high for low retardation potentials. Consequently, a distribution with respect to retardation potential is observed. Having differentiated the electron current, the energy spread is determined using the full width half maximum as observed in figure 1.5.2.2.

A typical energy spectrum obtained by de Jonge et al is shown in figure 1.5.2.3a [47]. In this figure, the values of d and T are 0.25 ± 0.01 eV and 588 ± 50 K respectively. Figure 1.5.2.3b compares the measured tunnelling parameter with theory. Numerically calculated curves of d versus I both overlapped very well with the measurements showing that the data was consistent with the FN model. The value of d increases with decreasing R for a given current, I . Consequently, it was determined that CNTs with radii larger than 1 nm were required, since it would not be possible to obtain sufficient beam current whilst still maintaining a small energy spread.

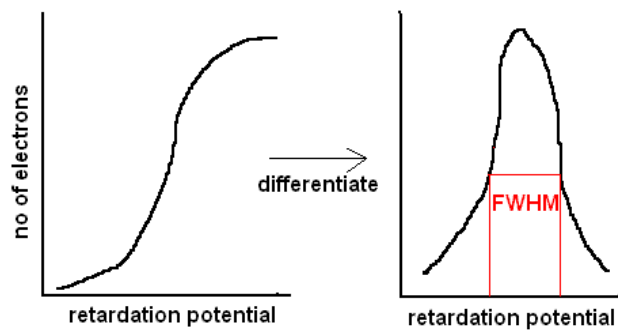


Figure 1.5.2.2: Graphs showing the relation between electron count and the full-width half maximum (FWHM) which determines the energy spread, ΔE .

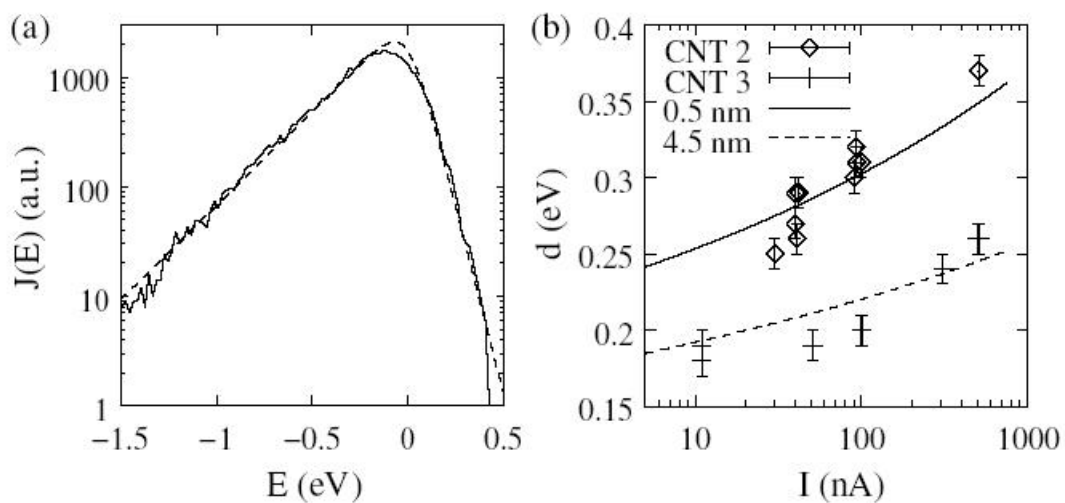


Figure 1.5.2.3: (a) Energy spectrum of a CNT recorded at 350 V and 30 nA, and fit with the FN theory (dashed). (b) Tunnelling parameter d as function of I for two CNTs, compared with numerically calculated curves [47]. Figure courtesy of De Jonge et al.

1.5.3 EMISSION STABILITY

The relationship between a material's properties and the stability of emission for a field emitter can be explained with the FN model of equation 1.5.1.1. Current fluctuations have two major causes:

- Variations in F
- Variations in ϕ

Due to the exponent in equation 1.5.2.1, I is extremely sensitive to variations in F or ϕ ; a 1% in ϕ or F can change can lead to a 15% change in I . Local changes in F are likely to occur as a result of geometric changes of the tip caused by surface migration and ion bombardment [50]. Also, ϕ is sensitive to adsorbates on the surface (which is the principle on which the ZrO Schottky emitter operates); a 25% change in ϕ can lead to a two orders of magnitude change in I . Despite ultra-high vacuum operation with a fully baked out field emitter, a layer of adsorbates forms after approximately 30 minutes followed by adsorption, vaporizing and molecular flow which can occur at room temperature. Flashing, which is the quick heating of the emitter, is performed regularly and operated under extremely good vacuum conditions ($< 10^{-10}$ mBar) with electronic feedback loops to stabilize the current [50]. The CNT, being a highly crystalline covalent structure [2], does not suffer from surface migration, which is typically observed on metal-bonded tungsten emitters, because the bond strength is much higher. Hence, the CNT can be operated at a few hundred degrees Celsius to continuously clean the emitter through desorption. Therefore, it was found that the vacuum requirements for the CNT emitter could be relaxed in comparison to that required for metal emitters.

The CNTs measured were constantly heated at 800 K during emission to avoid contamination. The probe current, I_p , was collected in a Faraday cup which was connected to a precision amplifier as shown in figure 1.5.3a. The extractor electrode was grounded and the emitter biased negatively at high voltage. The current-measuring electrode in the Faraday cup was biased positively to prevent current loss by secondary electron emission. Figure 1.5.3b shows that the emitted current has a

maximal drift of 1.5% over 1 hour. The drift is probably caused by a small drift of the temperature. The short-term peak to peak fluctuations were smaller than 0.2%.

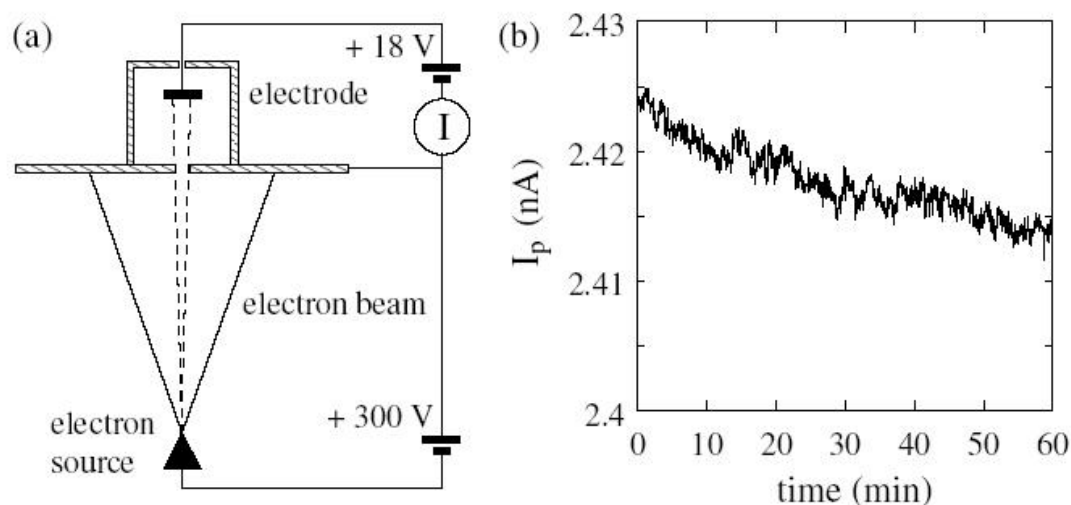


Figure 1.5.3: Measurements of the emission stability of a typical CNT. (a) The probe current was measured using a Faraday cup with a biased electrode placed above the electron source. (b) The probe current I_p measured as a function of time at $U = 270$ V, $I = 190$ nA, $T = 800$ K and a vacuum level of 2×10^{-10} torr. Figure courtesy of de Jonge.

1.5.4 THE VACUUM LEVEL

The vacuum level is important for noise calculations [49], because the higher the pressure, the more noise there will be. De Jonge et al found that the noise level increased to beyond the pixel threshold (of 256 grey levels) at 3×10^{-8} mBar.

1.5.5 SOURCE BRIGHTNESS

The most important parameter of an electron source is its brightness. The brightness is usually normalised on U , the electron energy at which the brightness is measured, resulting in the reduced brightness, B_r :

$$B_r = \frac{dI}{d\Omega} \frac{1}{\pi r_v^2} \frac{1}{U} = \frac{I_r'}{\pi r_v^2} \quad \text{Eq. 1.5.5}$$

with the reduced angular current density I_r' and r_v , the radius of the virtual source. For a focusing system, the reduced brightness indicates the amount of current, which can be focused into a spot of certain size and electron beam energy.

The virtual source size was found to roughly equal the radius of the CNT which was consistent with other work in this area [51]. Measurements of the reduced brightness were made for certain ΔE values to obtain the total figure of merit which is shown in figure 1.5.5. It shows that the majority of CNT sources tested were brighter at constant ΔE , and that they have a smaller ΔE for the equivalent brightness in a Schottky emitter.

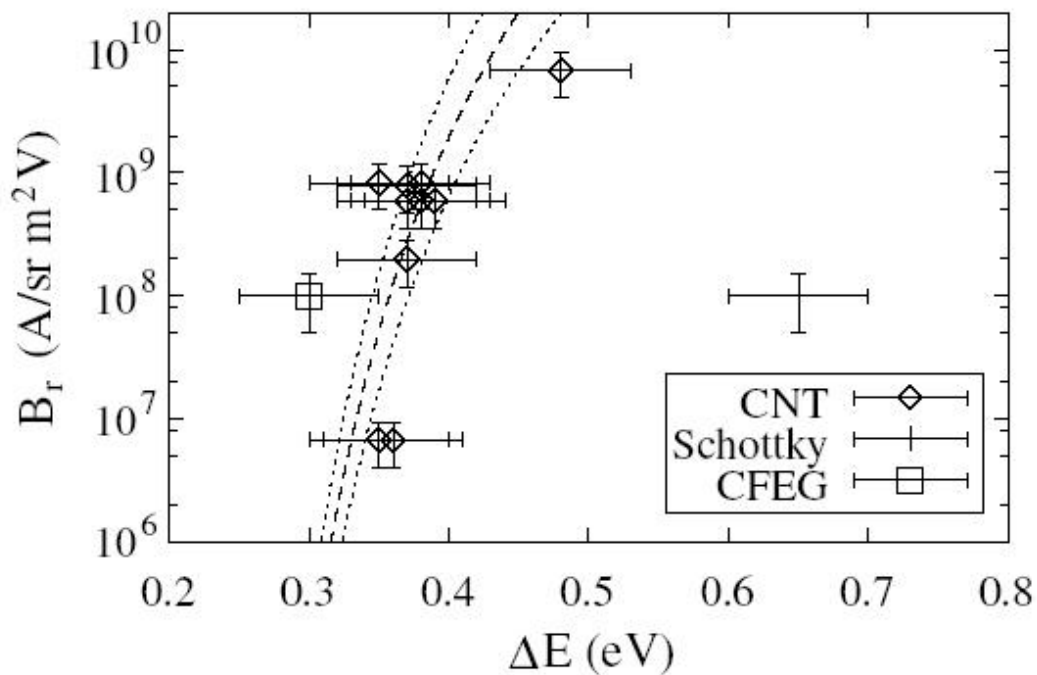


Figure 1.5.5: Reduced brightness B_r as a function of the energy spread ΔE measured for several CNTs at currents of 10-500 nA and temperatures of 600-700 K and calculated curve (dashed) and error range (dotted). The data of the Schottky emitter and the CFEG are also included.

1.5.6 SOURCE LIFETIME AND FAILURE MECHANISMS

The lifetime of an individual CNT electron source can be long: many hundreds of hours [52, 53]. For example, De Jonge et al have stated that their CNTs have lasted over 16 months without damage at a current of 100 nA, a vacuum level of 2×10^{-10} mbar and at a temperature of about 800 K.

However, the range of lifetimes for CNTs is large, so whilst CNTs can last a long time, some can fail after a few hours of field emission. The phenomena causing the degradation of the emitters are not completely understood presently. A combination of several factors plays a role.

Electrostatic deflection or mechanical stresses can cause alterations in the shape and surroundings of the emitter. This can lead to a decrease in local field amplification.

High currents can also damage a nanotube rapidly. A gradual decrease in field enhancement due to field evaporation was found in SWNTs when the emitted current was increased beyond certain limits (ranging from 300 nA to 1 μ A) [54]. For multi-walled CNTs, a shortening of the emitter over time [55] or damage to the outer walls of the nanotube due to high currents [56] has also been reported. Graphene layers or caps are removed, peeled back, or the end of the tube loses its graphitic structure and becomes amorphous [56,57]. MWNTs can be operated at total currents of up to 10 μ A, but the current should be kept below 1 μ A for stable operation and long life-time [51].

Following any type of degradation, a strong decrease in the emission current is observed and the voltage required to obtain comparable currents is substantially higher following such an episode.

1.6 SUMMARY

The combination of this data indicates that the CNT is a potentially powerful source for low-voltage, high resolution electron imaging equipment and research into a feasible fabrication method is the basis of this PhD.

Although there has been much research into field emission from carbon nanotubes, measurements have mainly focused on the maximum current density that can be obtained from nanotubes – research that is targeted towards field emission displays and microwave amplifiers. The research that exists on using carbon nanotubes as field emission sources is relatively small and focuses on carbon nanotubes attached to a tip. Although existing data is useful in giving an indication as to how a CNT source would behave, it does not provide data for a device that can be manufactured on a larger scale and with reproducible characteristics. There is no data on field emission from CNTs grown directly onto a tungsten tip, so it is of interest to see how the characteristics of CNTs grown in this way compare to CNTs attached. For instance, does lifetime increase? Are they easier to handle? Is alignment better? Are they brighter, more stable, and do they have a lower or higher energy spread? These are some of the questions that this thesis answers.

The second chapter will discuss techniques that have been employed to grow CNTs and to manipulate them so that they can be used as field emission sources. It will also detail various options open to the author and describe the results together with their relative merits. The third chapter details the method settled upon which is to grow CNTs directly onto the apex of existing tungsten electron sources and discusses yield, reproducibility and robustness. The fourth chapter provides a detailed investigation of the field emission characteristics of the CNT, paying particular attention to stability and its definition, together with energy spread and brightness measurements. The fifth chapter observes the performance of CNT electron sources in an electron microscope, indicating their superior performance in terms of resolution, brightness and virtual source size. The final chapter summarizes the work in this thesis and proposes where research in this area should go in the future.

1.7 REFERENCES

- [1] S. Iijima, Nature 354, 56 (1991).
- [2] Niels de Jonge and Jean-Marc Bonard, Phil. Trans. R. Soc. Lond. A 362, 2239–2266 (2004).
- [3] Y. Saito, T Yoshikawa, S. Bandow, M. Tomita and T. Hayashi, Phys. Rev. B 48, 1907 (1993).
- [4] M. Endo, K. Takeuchi, T. Hiraoka, T. Furuta, T. Kasai, X. Sun, C.H. Kiang, and M.S. Dresselhaus, J. Phys. Chem. Solids 58, 1707 (1997).
- [5] C.H. Kiang, M. Endo, P.M. Ajayan, G. Dresselhaus and M.S. Dresselhaus, Phys. Rev. Lett. 81, 1869 (1998).
- [6] A. Bachtold, C. Strunk, J.P. Salvelat, J.M. Bonard, L. Forro, T. Nussbaumer, C. Schonenberger, Nature 397, 673 (1999).
- [7] W. I. Milne, K. B. K. Teo, G. A. J. Amaratunga, P. Legagneux, L. Gangloff, J.-P. Schnell, V. Semet, V. Thien Binh and O. Groening, J.Mater. Chem., 14, 1–12, 2004.
- [8] H.J. Qi, K.B.K. Teo, K.K.S. Lau, M.C. Boyce, W.I. Milne, J. Robertson and K.K. Gleason, "*Determination of mechanical properties of carbon nanotubes and vertically aligned carbon nanotube forests using nanoindentation*" Journal of Mechanics and Physics of Solids 51, 2213 (2003)
- [9] J. Li, R. Stevens, L. Delzeit, H.T. Ng, A. Cassell, J. Han and M. Meyyappan, "Electronic Properties of Multiwalled Carbon Nanotubes in an Embedded Vertical Array", Applied Physics Letters, Vol. 81 (5), pp. 910-912 (2002).
- [10] H.J. Qi, K.B.K. Teo, K.K.S. Lau, M.C. Boyce, W.I. Milne, J. Robertson and K.K. Gleason, "*Determination of mechanical properties of carbon nanotubes and vertically aligned carbon nanotube forests using nanoindentation*" Journal of Mechanics and Physics of Solids 51, 2213 (2003)
- [11] J. Li, R. Stevens, L. Delzeit, H.T. Ng, A. Cassell, J. Han and M. Meyyappan, "Electronic Properties of Multiwalled Carbon Nanotubes in an

- Embedded Vertical Array", *Applied Physics Letters*, Vol. 81 (5), pp. 910-912 (2002).
- [12] K.B.K. Teo, C. Singh, M. Chhowalla, W.I. Milne, *Encyc. Nanosci. Nanotech.* X Pg 1-22, 2003.
- [13] A. Bachtold, P. Hadley, T. Nakamishi, C. Dekker, *Science* 294, 1317 (2001).
- [14] S.J. Tans, A.R.M. Verschueren, C. Dekker, *Nature* 393, 49 (1998).
- [15] R. Martel, T. Schmidt, H.R. Shea, T. Hertel, P. Avouris, *Appl. Phys. Lett.* 73, 2447 (1998).
- [16] V. Derycke, R. Martel, J. Appenzeller, P. Avouris, *Nano. Lett.* 1, 453 (2001)
- [17] J. Kong, N.R. Franklin, C.W. Zhou, M.G. Chapline, S. Peng, K.J. Cho H.J. Dai, *Science* 287, 6212 (2000).
- [18] P.G. Collins, K. Bradley, M. Ishigami, A. Zettl, *Science* 287, 1801 (2000)
- [19] K. Tsukagoshi, B.W. Alphenaar, H. Ago, *Nature* 401, 572 (1999).
- [20] T.W. Tombler, C.W. Zhou, L. Alexseyev, J. Kong, H.J. Dai, L. Lei, C.S. Jayanthi, M.J. Tang, S.Y. Wu, *Nature* 405, 769 (2000).
- [21] R.H. Baughman, A.A. Zakhidov, W.A. de Heer, *Science*, 280, 1744 (1998).
- [22] J. Li, R. Stevens, L. Delzeit, H.T. Ng, A. Cassell, J. Han, M. Meyyappan, *Appl. Phys. Lett.* 81, 910 (2002).
- [23] S. Musso, S. Porro, M. Rovere, A. Tagliaferro, E. Laurenti, M. Mann, K.B.K. Teo, W.I. Milne. *Diamond & Related Materials* 15, 1085 – 1089 (2006).
- [24] M. Hirscher, M. Becher, M. Haluska, U. Dettlaff-Weglikowska, A. Quintel, G.S. Deusberg, Y.M. Choi, P. Downer, M. Hulman, S. Roth, I. Stepanek, P. Bernier, *Appl. Phys. A* 72, 129 (2001).
- [25] P. Calvert, *nature* 399, 210 (1999).
- [26] Deuk-Seok Chung, S. H. Park, H. W. Lee, J. H. Choi, S. N. Cha, J. W. Kim, J. E. Jang, K. W. Min, S. H. Cho, M. J. Yoon, J. S. Lee, C. K. Lee, J. H. Yoo, Jong-Min Kim, J. E. Jung, Y. W. Jin, Y. J. Park, and J. B. You, *Appl. Phys. Lett.* 80, 4045 (2002).

- [27] K.B.K. Teo, E. Minoux, L. Hudanski, F. Peauger, J.-P. Schnell, L. Gangloff, P. Legagneux, D. Dieumgard, G.A.J. Amaratunga and W.I. Milne. "Microwave Devices: Carbon Nanotubes as Cold Cathodes", *Nature* 437, 968 (2005).
- [28] N. de Jonge, M. Allieux, J.T. Oostveen, K.B.K. Teo and W.I. Milne. "Optical performance of carbon nanotube electron sources", *Physical Review Letters* 94, 186807 (2005).
- [29] W.I. Milne, K.B.K. Teo, E. Minoux, O. Groening, L. Gangloff, L. Hudanski, J.-P. Schnell, D. Dieumgard, F. Peauger, I.Y.Y. Bu, M.S. Bell, P. Legagneux, G. Hasko, and G.A.J. Amaratunga "Aligned carbon nanotube/fibers for applications in vacuum microwave amplifiers", *Journal of Vacuum Science and Technology B* 24, 345 (2006).
- [30] Thesis K.B.K. Teo, Cambridge University, 2002.
- [31] S. T. Purcell, P. Vincent, C. Journet, and Vu Thien Binh, *Phys. Rev. Lett.* 88, 105502 (2002).
- [32] Rinzler, A. G., Hafner, J. H., Nikolaev, P., Lou, L., Kim, S. G., Tomanek, D., Nordlander, P., Colbert, D. T. & Smalley, R. E. 1995 Unraveling nanotubes: field emission from an atomic wire. *Science* 269, 1550–1553.
- [33] T. Utsumi, *IEEE Trans. Electron Dev.* 38, 2276 (1991).
- [34] Y. Wei, C. Xie, K. A. Dean, and B. F. Coll, *Appl. Phys. Lett.* 79, 4527 (2001).
- [35] Paulmier, T., Balat-Pichelin, M., Le Queau, D., Berjoan, R. & Robert, J. F. 2001 Physicochemical behavior of carbon materials under high temperature and ion radiation. *Appl. Surf. Sci.* 180, 227–245.
- [36] Sources for pictures:
- (a), (b): www.sidiamond.com, under ANI (Applied Nanotech Inc)
- (c), (d): www.oxfordxtg.com
- (e): W. B. Choi, D. S. Chung, J. H. Kang, H. Y. Kim, Y. W. Jin, I. T. Han, Y. H. Lee, J. E. Jung, N. S. Lee, G. S. Park, and J.M. Kim, *Appl. Phys. Lett* 75, 3129 (1999).

- (f): Deuk-Seok Chung, S. H. Park, H. W. Lee, J. H. Choi, S. N. Cha, J. W. Kim, J. E. Jang, K. W. Min, S. H. Cho, M. J. Yoon, J. S. Lee, C. K. Lee, J. H. Yoo, Jong-Min Kim, J. E. Jung, Y. W. Jin, Y. J. Park, and J. B. You, *Appl. Phys. Lett.* 80, 4045 (2002).
- [37] Choi, W. B. (and 10 others) 1999 Fully sealed, high-brightness carbon-nanotube field-emission display. *Appl. Phys. Lett.* 75, 3129–3131.
- [38] Saito, Y. & Uemura, S. 2000 Field emission from carbon nanotubes and its application to electron sources. *Carbon* 38, 169–182.
- [39] Chung, D. S., Choi, W. B., Kang, J. H., Kim, H. Y., Han, I. T., Park, Y. S., Lee, Y. H., Lee, N. S., Jung, J. E. & Kim, J. M. 2000 Field emission from 4.5 in. single-walled and multiwalled carbon nanotube films. *J. Vac. Sci. Technol. B* 18, 1054–1058.
- [40] L. Gangloff, E. Minoux, K. B. K. Teo, P. Vincent, V. T. Semet, V. T. Binh, M. H. Yang, I. Y. Y. Bu, R. G. Lacerda, G. Pirio, J. P. Schnell, D. Pribat, D. G. Hasko, G. A. J. Amaratunga, W. I. Milne, and P. Legagneux; *Nanoletters* 2004, Vol. 4, No. 9. 1575-1579.
- [41] Kenneth B. K. Teo, Eric Minoux, Ludovic Hudanski, Franck Peauger, Jean-Philippe Schnell, Laurent Gangloff, Pierre Legagneux, Dominique Dieumegard, Gehan A. J. Amaratunga, William I. Milne; *Nature* Vol. 437, 2005, 968.
- [42] Sugie, H., Tanemure, M., Filip, V., Iwata, K., Takahashi, K. & Okuyama, F. 2001 Carbon nanotubes as electron source in an X-ray tube. *Appl. Phys. Lett.* 78, 2578–2580.
- [43] Marcuccio, S., Genovese, A. & Andrenucci, M. 1997 FEED microthruster technology status and prospects. In *Proc. 48th Int. Astronautical Federation Cong.*, Turin, Italy. Paris: International Astronautical Federation.
- [44] Applied Physics Technologies brochure, 1600 NE Miller St. McMinnville, OR 97128, 2005.
- [45] FEI Company brochure, 5350 NE Dawson Creek Dr. Hillsboro, OR 97124 USA, 2005.
- [46] Martijn Fransen, *Towards high-brightness, monochromatic electron sources*, Technische Universiteit Delft/ Philips NatLab Promotie: 9 Februari 1999

- [47] N. de Jonge, M. Allieux, J.T. Oostveen, K.B.K. Teo and W.I. Milne. "Optical performance of carbon nanotube electron sources", *Physical Review Letters* 94, 186807 (2005).
- [48] R. H. Fowler and L. Nordheim. Electron emission in intense electric fields. *Proc. Roy. Soc. London A*, 119:173-181, 1928.
- [49] N. de Jonge, M. Allieux, M. Doytcheva, M. Kaiser, K.B.K. Teo, R.G. Lacerda and W.I. Milne. "Characterization of the field emission properties of individual thin carbon nanotubes", *Applied Physics Letters* **85**, (2004).
- [50] J. F. Hainfield. Understanding and using field emission sources. *Scanning Electron Microscopy*, 1:591-604, 1977.
- [51] N. de Jonge. The brightness of carbon nanotube electron emitters. *J. Appl. Phys*, 95:673-681, 2004.
- [52] Dean, K. A. & Chalamala, B. R. 1999 The environmental stability of field emission from single-walled carbon nanotubes. *Appl. Phys. Lett.* 75, 3017–3019.
- [53] Fransen, M. J., van Rooy, T. L. & Kruit, P. 1999 Field emission energy distributions from individual multiwalled carbon nanotubes. *Appl. Surf. Sci.* 146, 312–327.
- [54] Dean, K. A., Burgin, T. P. & Chamala, B. R. 2001 Evaporation of carbon nanotubes during electron field emission. *Appl. Phys. Lett.* 79, 1873–1875.
- [55] Wei, Y. Y., Dean, K. A., Coll, B. F. & Jaskie, J. E. 2001 Stability of carbon nanotubes under electric field studied by scanning electron microscopy. *Appl. Phys. Lett.* 79, 4527–4529.
- [56] Wang, Z. L., Poncharal, P. & de Heer, W. A. 2002 In situ imaging of field emission from individual carbon nanotubes and their structural damage. *Appl. Phys. Lett.* 80, 856–858.
- [57] Wang, Z. I., Poncharal, P. & de Heer, W. A. 2000 Nanomeasurements in transmission electron microscopy. *Microsc. Microanalysis* 6, 224–230.